International Journal of
Molecular Sciences

MDPI

Supplementary Figures

Figure S1:
Schematic representation of epitope extraction via SPR chip in combination with MALDI MS. Sample injection over the SPR gold chip with the antibody immobilized on one channel. Peptides are injected over the antibody channel allowing the SPR sensorgram recording of the binding peptides and the MALDI-MS of the eluted epitope peptides. The K_D of the intact protein is measured by injecting a dilution series of the intact protein only over the SPR chip.
Figure S2:
Schematic representation of epitope identification by epitope excision–mass spectrometry. After the protein–antibody complex is formed, a protease is added to the complex. The epitope peptide is shielded by the antibody from proteolytic digestion, and can be eluted after washing of non-binding peptides.
Figure S3:
Affinity captured antibody for column preparation with Sepharose immobilized protein G crosslinked to the Fc antibody region.
Figure S4:
Mass spectrometric determination of intact apomyoglobin, average mass 16952.49 Da. A. MALDI-MS of singly, doubly and triply charged protein. B. ESI-MS of multiply charged intact protein.
Figure S5:
MALDI-MS measurements of digested myoglobin. A. MALDI-MS spectra of myoglobin tryptic peptides digested at atmospheric pressure for 18 hours. B. MALDI-MS spectra of tryptic peptides digested with cyclic high pressure technology for 2 hours.
Figure S6:
Crystal structure of Adalimumab Fab (blue and green) in complex with TNF-α(orange). The identified epitope (Adalimumab heavy chain 12-29) is marked in red.
Figure S7:
IL8 3D structure depicting epitope identification. (A) Epitope peptides [12–20] and [55–60] highlighted (red) in the 3D-structure of IL8. (B) Binding sites of IL8 (blue) to CXCR1. (C) Overlapping region of the antibody epitope and the receptor binding site on IL8.
Figure S8:
Epitope extraction applied to IL8 and anti-IL8 antibody. (A) Experimental procedure of the SPR based epitope extraction. (B) Experimental procedure of the micro affinity column based epitope extraction.
Figure S9:
SPR sensorgram of the interaction between intact α-Galactosidase (A)/epitope peptide [309–332] (B) and anti-α-Galactosidase antibody. K_D calculation was performed from three concentrations of intact α-Galactosidase; B, K_D calculation from four concentrations of epitope peptide [309-332] .
Figure S10:
Schematic representation of the SELEX procedure for preparation of affinity-optimized
DNA-aptamers.
Figure S11:
I-Tasser predicted ribbon representation of the structure of C-Met protein. Represented in yellow is the extracellular domain (1-932) of the protein fused with a C-terminal polyhistidine-tagged Fc region of human IgG 1. Glycosylation sites are depicted in red.
Figure S12:

Comparison of 3D structures depicting an aptamer–protein interaction (A) and antibody–protein interaction (B).

Figure S13:

C-Met 3D structure depicting epitope identification. The epitope peptides for CLN0003 and CLN00004 aptamers are highlighted (Blue and light Blue) in the 3D-structure of C-Met.

Figure S1

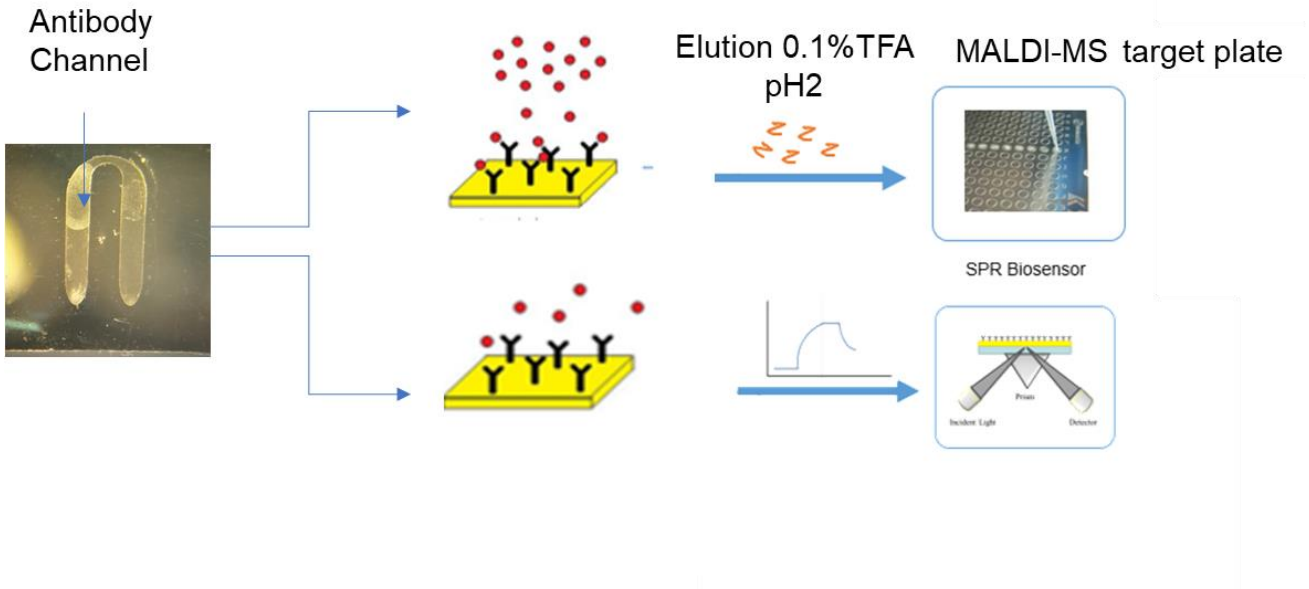

Figure S2

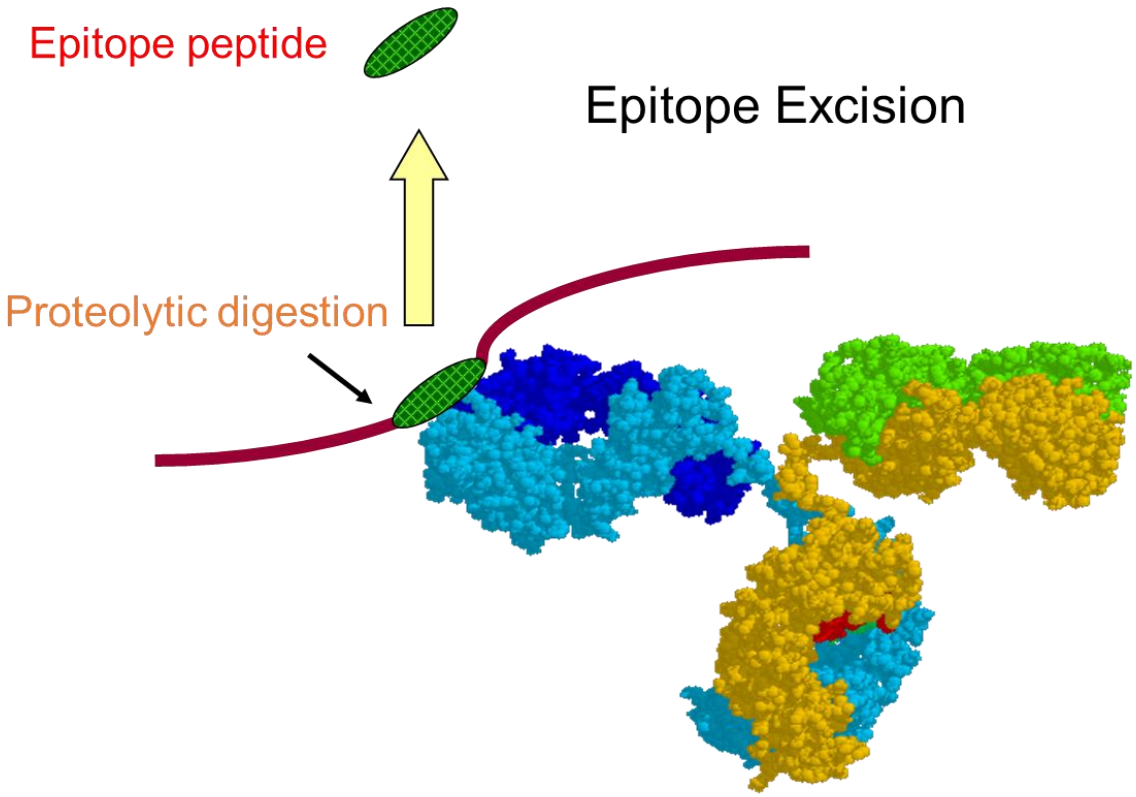

Figure S3

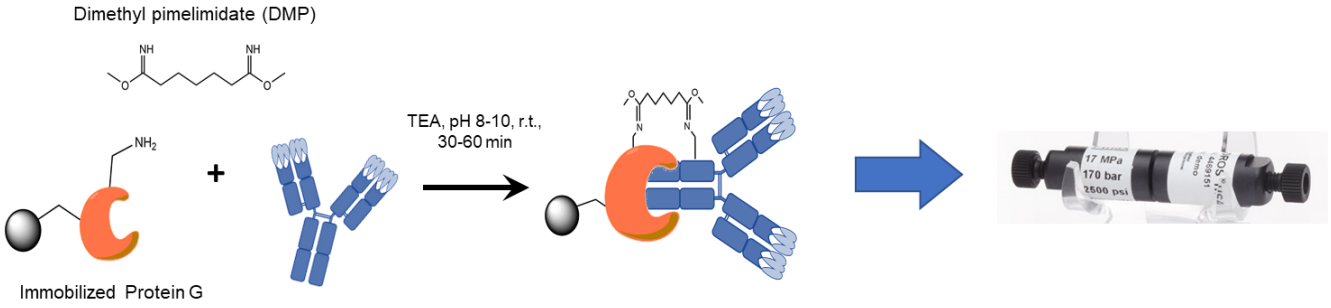
Dimethyl pimelimidate (DMP)
NH
NH
O
O
NH2
+
TEA, pH 8-10, r.t.,
30-60 min
N
N
O
O
17 MPa
170 bar
2500 psi
Immobilized Protein G

Figure S4

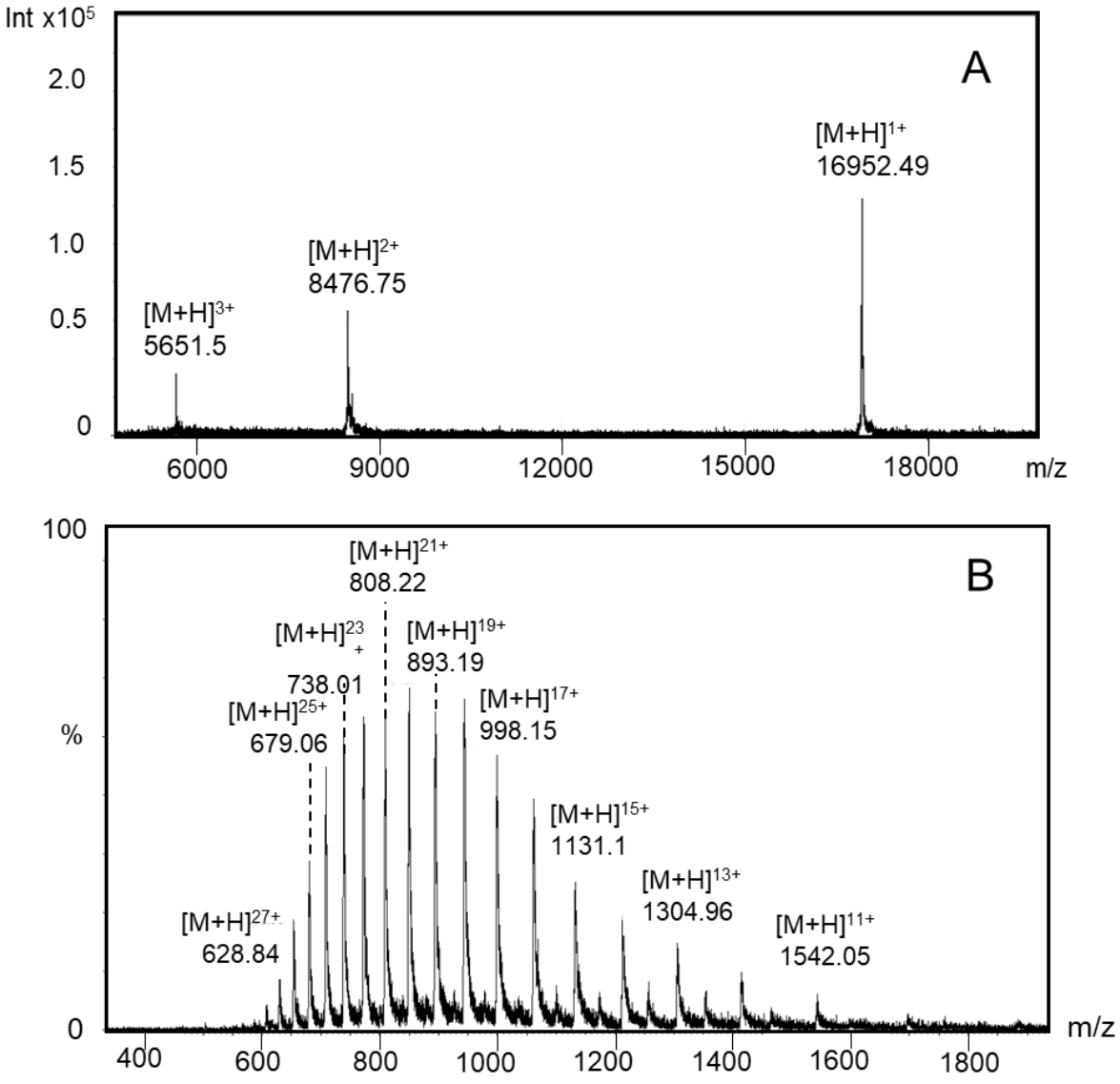
Int x10^5
2.0
1.5
1.0
0.5
0
A
[M+H]1+
16952.49
[M+H]2+
8476.75
[M+H]3+
5651.5
6000
9000
12000
15000
18000
m/z
100
%
0
B
[M+H]21+
808.22
[M+H]23+
738.01
[M+H]19+
893.19
[M+H]25+
679.06
[M+H]17+
998.15
[M+H]15+
1131.1
[M+H]13+
1304.96
[M+H]27+
628.84
[M+H]11+
1542.05
400
600
800
1000
1200
1400
1600
1800
m/z

Figure S5

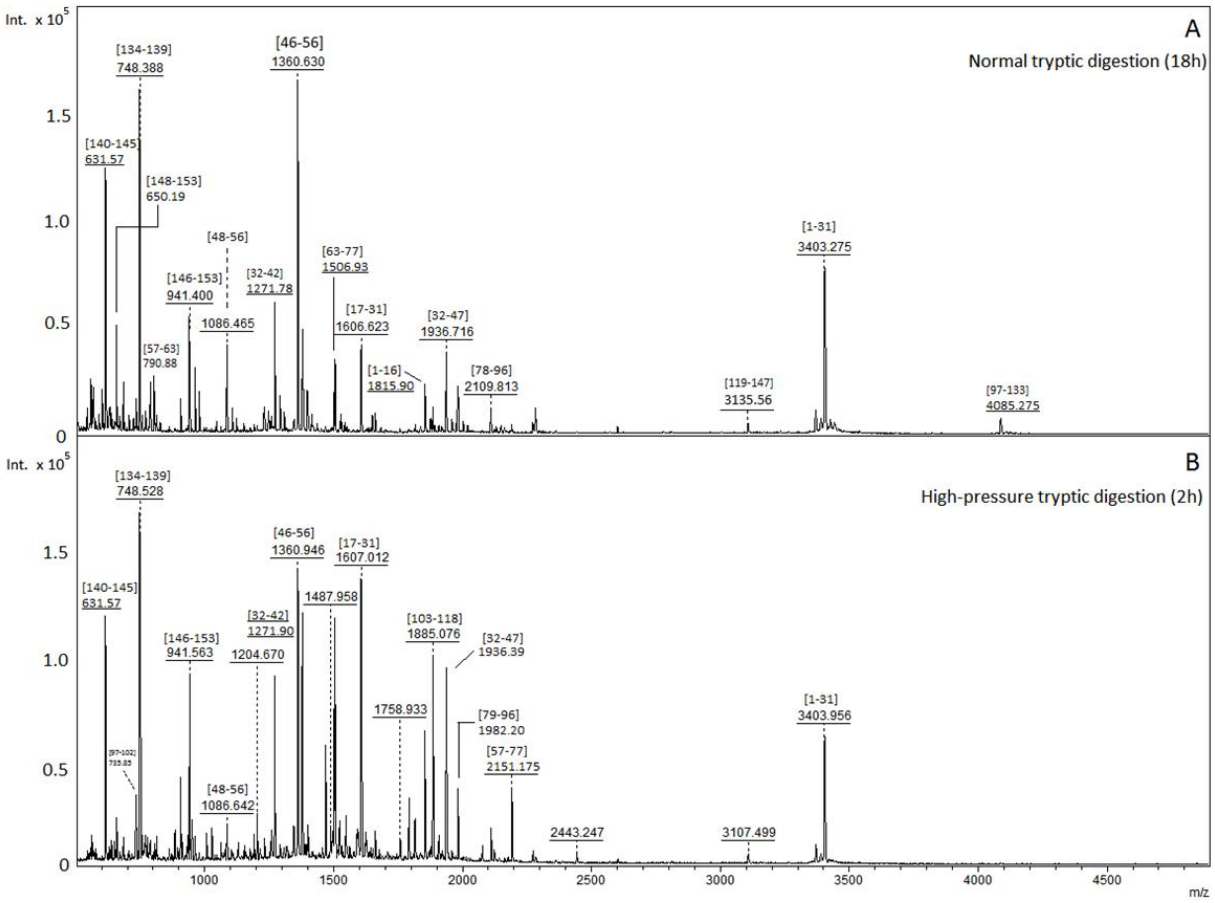
Int. x 10^5
A
Normal tryptic digestion (18h)
[134-139]
748.388
[46-56]
1360.630
[140-145]
631.57
[148-153]
650.19
[48-56]
[146-153]
941.400
[32-42]
1271.78
[63-77]
1506.93
[17-31]
1606.623
[32-47]
1936.716
[1-31]
3403.275
1086.465
[57-63]
790.88
[1-16]
1815.90
[78-96]
2109.813
[119-147]
3135.56
[97-133]
4085.275
Int. x 10^5
B
High-pressure tryptic digestion (2h)
[134-139]
748.528
[46-56]
1360.946
[17-31]
1607.012
[140-145]
631.57
1487.958
[32-42]
1271.90
[103-118]
1885.076
[146-153]
941.563
1204.670
[32-47]
1936.39
1758.933
[79-96]
1982.20
[1-31]
3403.956
[57-77]
2151.175
[48-56]
1086.642
2443.247
3107.499
0
0.5
1.0
1.5
1000
1500
2000
2500
3000
3500
4000
4500
m/z

Figure S6

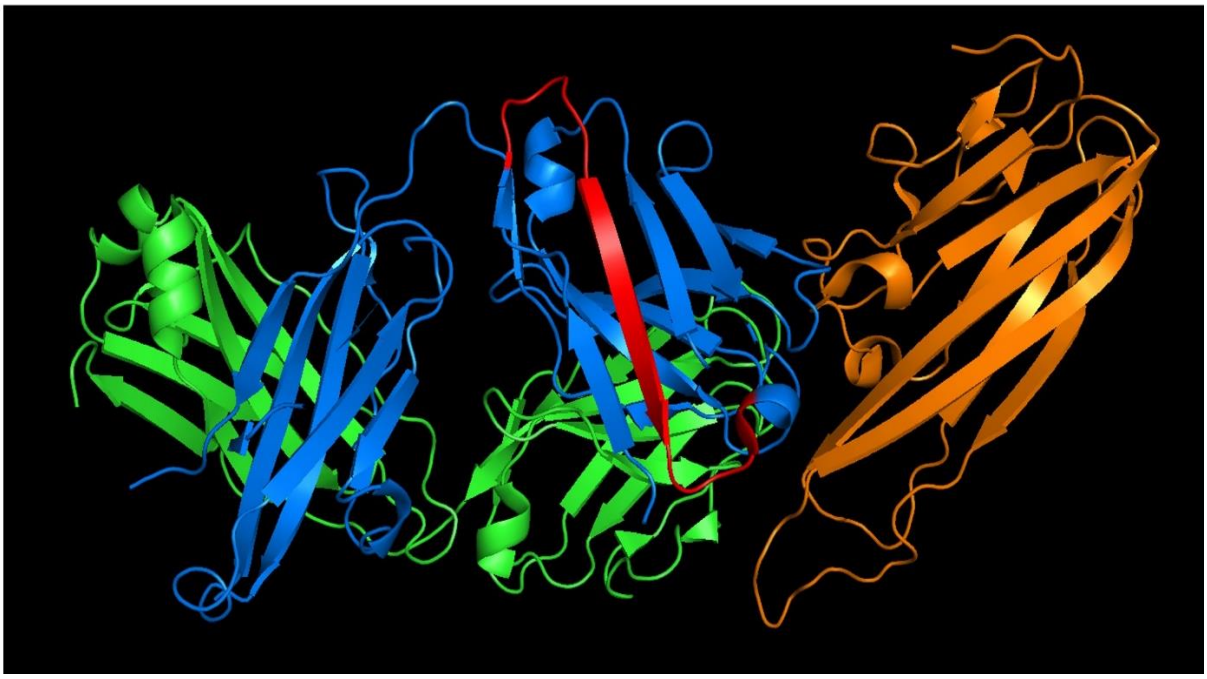

Figure S7

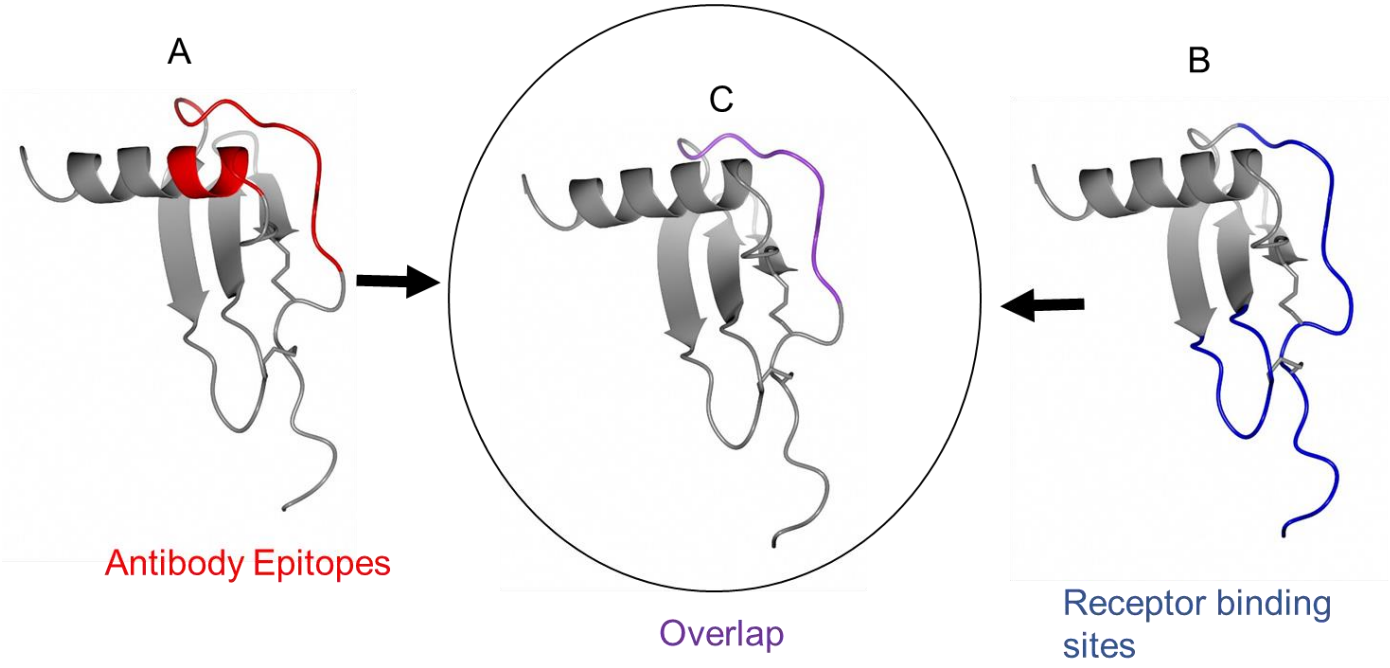

Figure S8

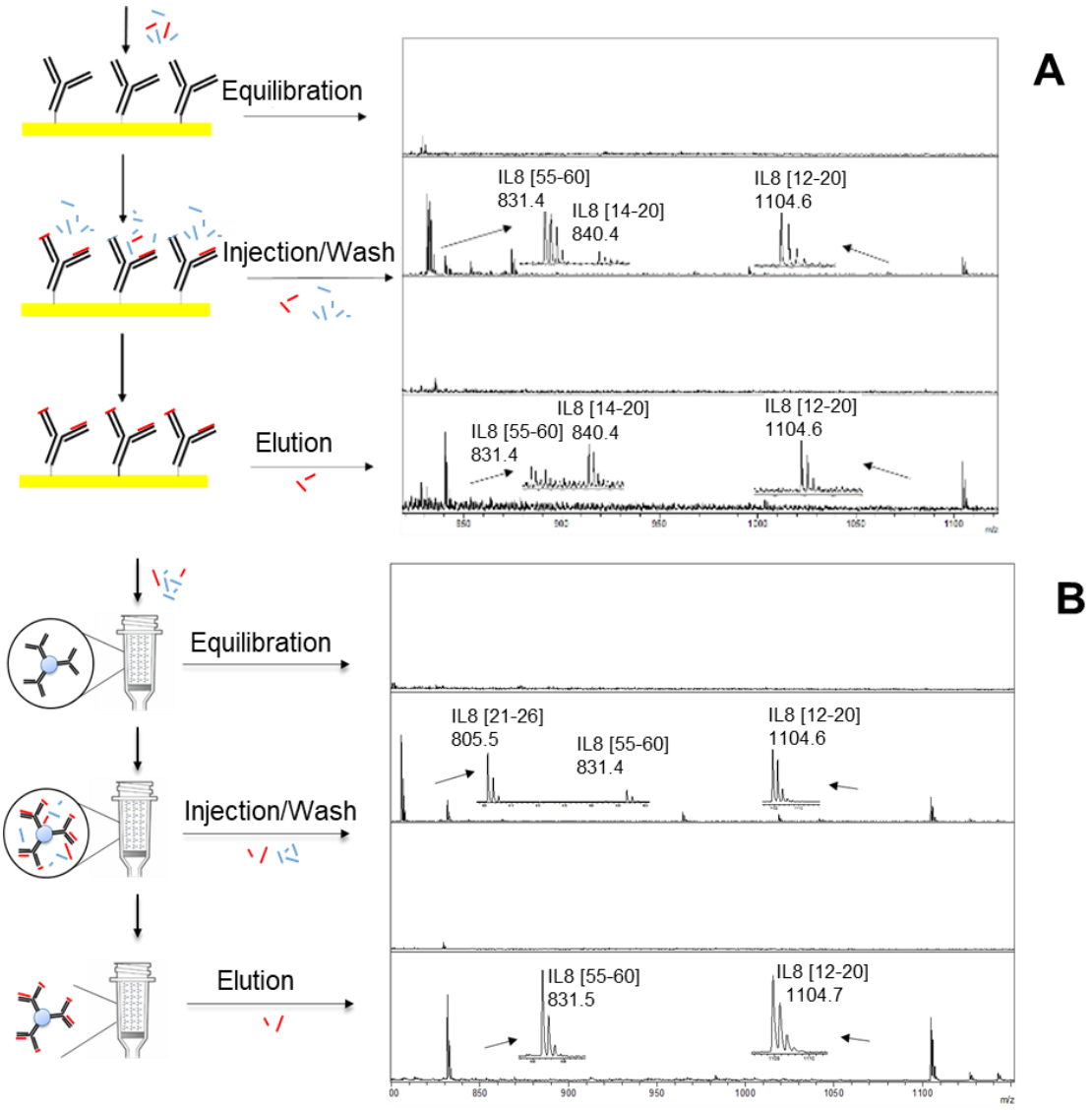
A
Equilibration
Injection/Wash
Elution
IL8 [55-60]
831.4
IL8 [14-20]
840.4
IL8 [12-20]
1104.6
IL8 [14-20]
840.4
IL8 [55-60]
831.4
IL8 [12-20]
1104.6
B
Equilibration
Injection/Wash
Elution
IL8 [21-26]
805.5
IL8 [55-60]
831.4
IL8 [12-20]
1104.6
IL8 [55-60]
831.5
IL8 [12-20]
1104.7
850
900
950
1000
1050
1100
m/z

Figure S9

A

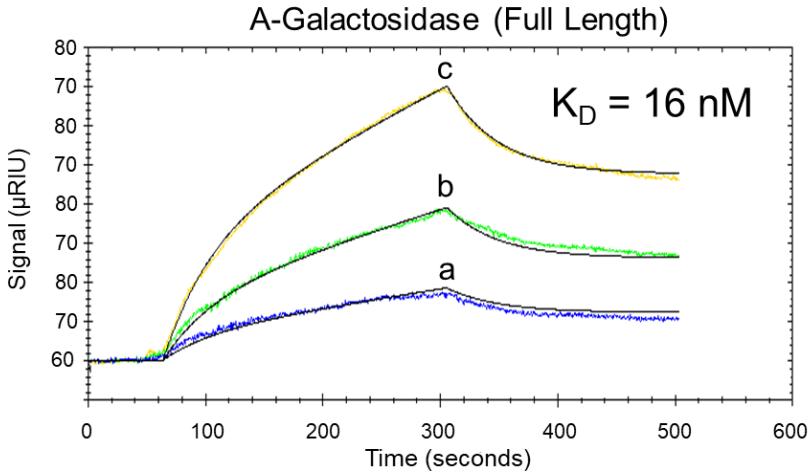

- a = 5 µM
- b = 10 µM
- c = 20 µM

B

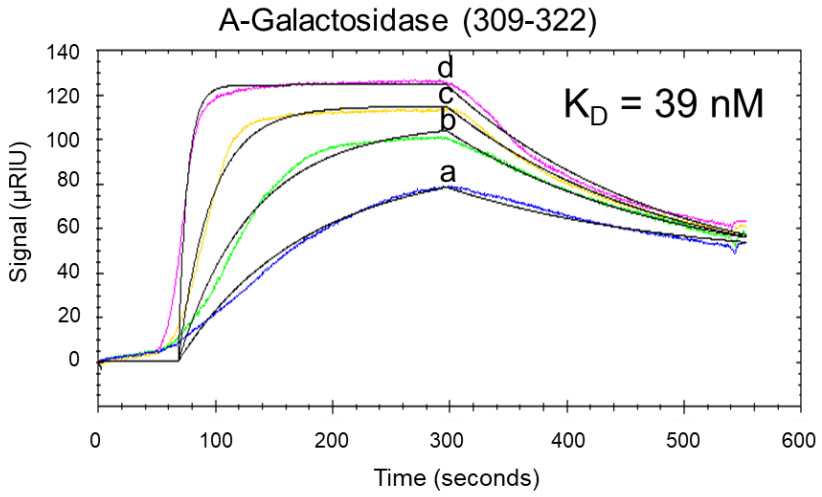

- a = 50 nM
- b = 100 nM
- c = 250 nM
- d = 1 µM

Figure S10

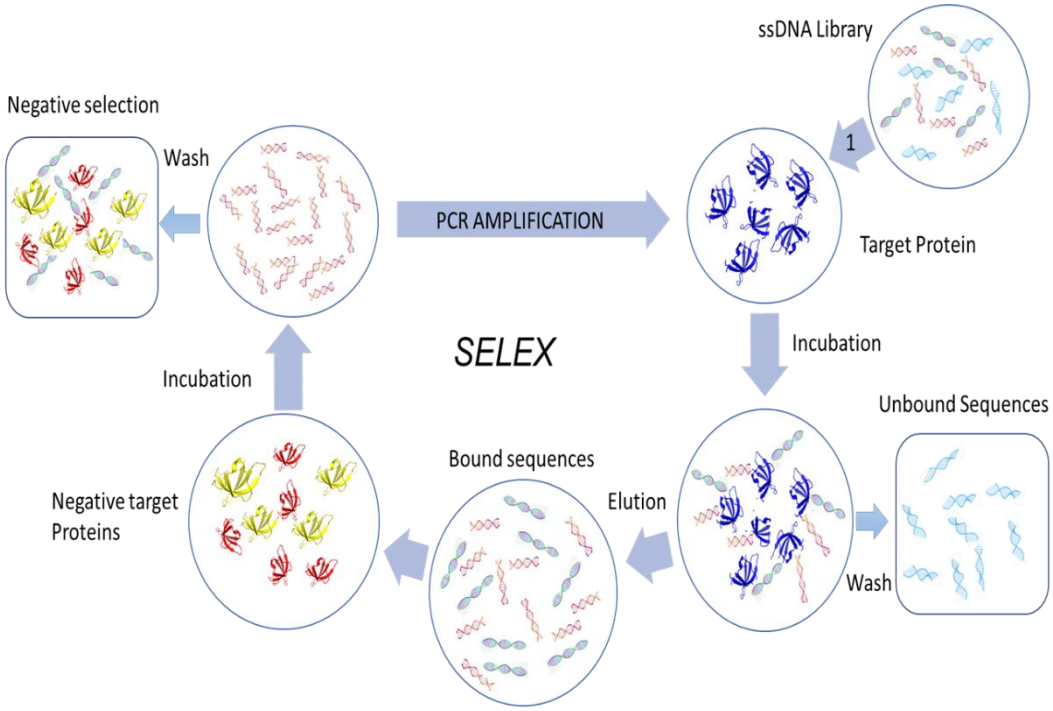
ssDNA Library
1
Target Protein
Incubation
Unbound Sequences
Wash
Elution
Bound sequences
Negative target
Proteins
Incubation
SELEX
PCR AMPLIFICATION
Wash
Negative selection

Figure S11

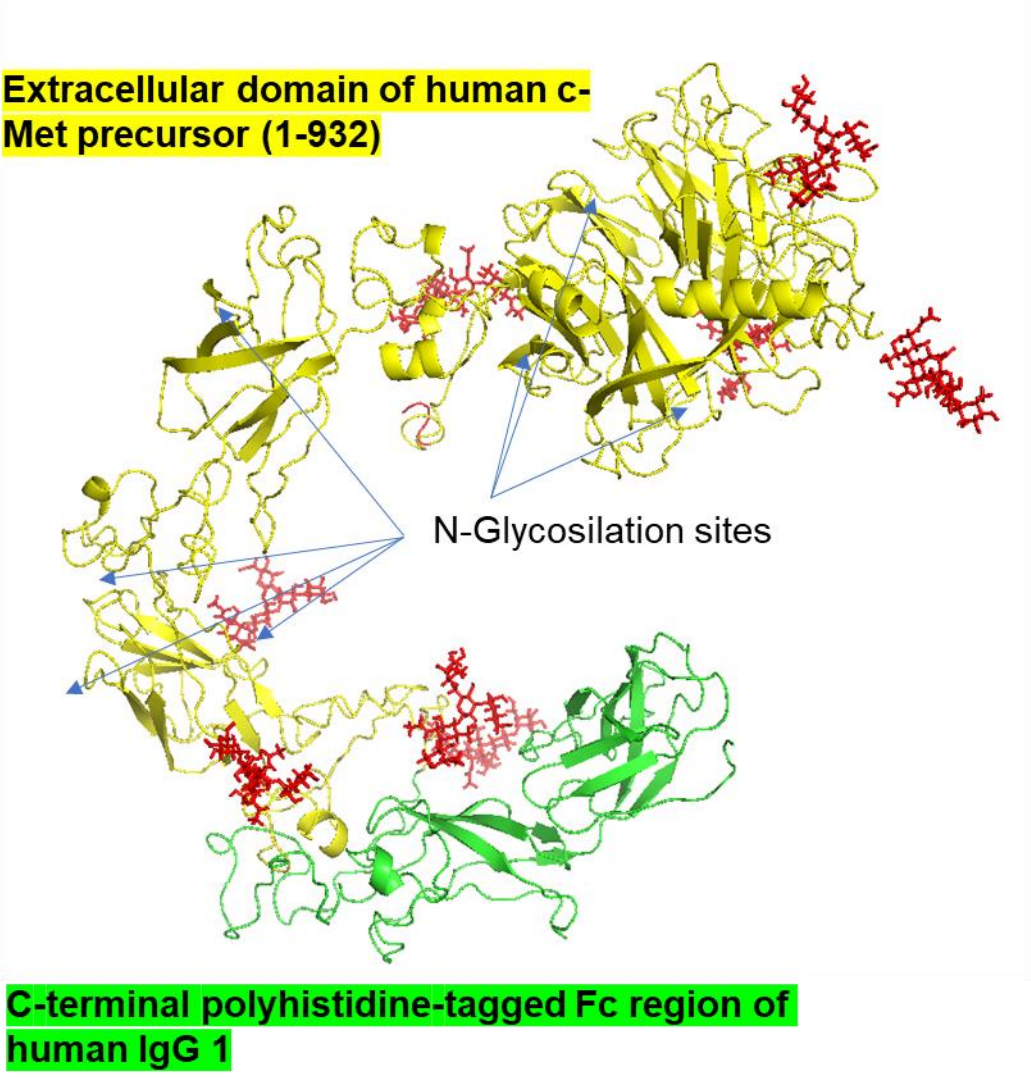
Extracellular domain of human c-Met precursor (1-932)
N-Glycosilation sites
C-terminal polyhistidine-tagged Fc region of human IgG 1

International Journal of
Molecular Sciences

MDPI

Figure S12

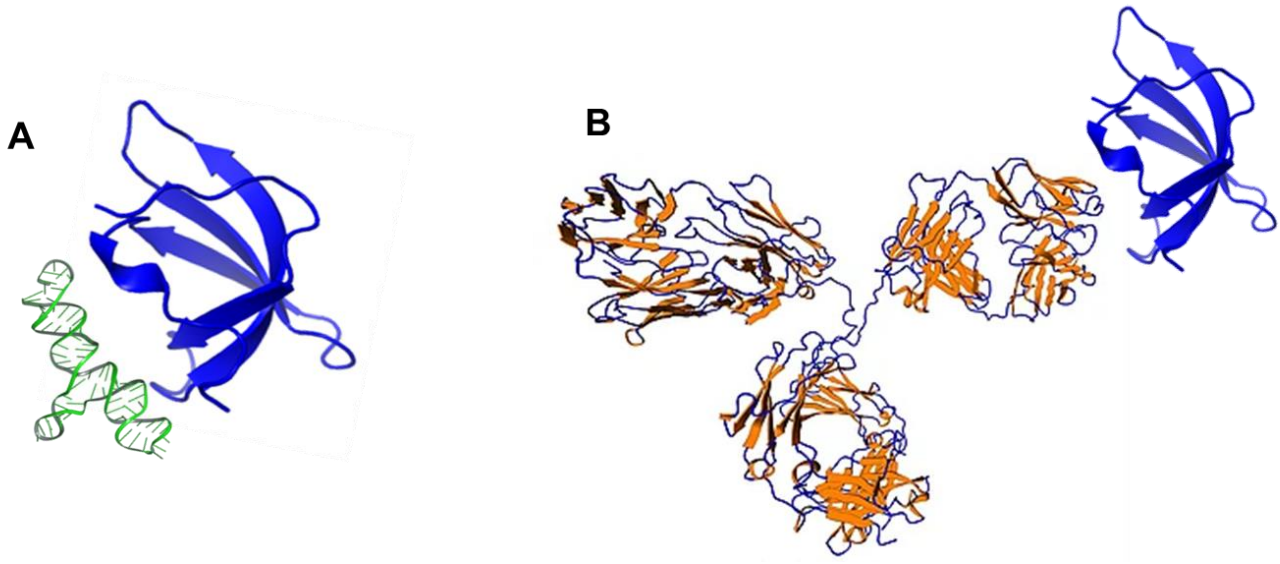

Figure S13